Analytic model and concise impedance boundary condition for viscous acoustics in ducted shear flow

Doran Khamis* and Edward J. Brambley†

University of Cambridge, UK

A weakly viscous mean flow boundary layer is sandwiched between an inviscid outer flow and a viscous sublayer to form an asymptotic patchwork model for ducted acoustics in shear flow over an acoustic lining. Analytical solutions are found for the acoustic mode shapes in the three regions and compared with solutions of the linearised compressible Navier–Stokes equations (LNSE). By asymptotically matching the analytical solutions, a closed-form effective impedance boundary condition is derived, applicable at the wall of an inviscid plug flow. Duct modes in the wavenumber and frequency domain are investigated and compared to the Myers boundary condition, its first order correction (the Modified Myers condition) and numerical solutions of the LNSE.

1. Introduction

The majority of work pertaining to the acoustics above an acoustic lining considers an inviscid fluid. Early work considered a uniform flow (e.g. [1,2]) or mean flow shear (e.g. [3–5]) and used numerical solutions of the linearised inviscid governing equations to find that acoustic linings can increase sound attenuation. Specifically, the wavenumber of a cuton duct mode in a lined duct is given a small nonzero imaginary part, such that in effect all modes are slightly cutoff and hence decay. More recent studies have shown that to accurately reproduce experimental results, viscosity must be taken into account [6,7].

Analytical studies of a sheared inviscid boundary layer above an acoustic lining have led to important predictions of the number of possible surface modes [8,9] (those modes that exist primarily very close to the lined wall, and decay exponentially into the duct). Stability analyses have shown that it is these surface modes that can lead to convective instabilities [9–11] which have also been identified in experiments [12,13]. Because acoustic liners can support surface modes where a hard wall can not, their use can lead to an amplification of noise as well as a reduction due to the possibility of an instability being triggered. Theoretical identification of these unstable modes is therefore of utmost importance. It is known that viscosity effects the stability behaviour of surface modes, and stabilises the system at small wavelengths [14], but compared to the inviscid case the viscous case is barely studied.

Viscosity has been included in a number of studies [15–17] aimed at deriving an effective impedance boundary condition (a modified lining impedance that accounts for viscosity in the boundary layer and may be applied at the wall of a uniform inviscid flow). In order to arrive at closed-form analytical solutions, these studies all make simplifying assumptions. Nayfeh in Ref. 15 considers only the acoustic boundary layer which is thin compared to the main flow boundary layer. In Ref. 16, only small changes in the velocity and temperature are allowed across the boundary layer, and the viscosity is chosen to be independent of the temperature. Brambley makes fewer simplifications in Ref. [17], but derives a system which models a vanishingly thin shear layer and which must be solved numerically; closed-form solutions are found in high and low frequency limits.

Without either making limiting simplifications or taking specific asymptotic limits, there is no known closed-form solutions for the acoustics in a finite-thickness sheared, viscous boundary layer. Reports, or approximations, of boundary layer thicknesses and Reynolds numbers of aeroengines – data which are few and far between – suggest that the boundary layer is thicker for a given Reynolds number than that which

*PhD Student, Department of Applied Mathematics and Theoretical Physics, University of Cambridge, Centre for Mathematical Sciences, Wilberforce Road, Cambridge CB3 0WA, United Kingdom. AIAA member.

†Research Fellow, Department of Applied Mathematics and Theoretical Physics, University of Cambridge, Centre for Mathematical Sciences, Wilberforce Road, Cambridge CB3 0WA, United Kingdom. AIAA member.

the Blasius scaling predicts. This could be, for example, due to a turbulent boundary layer where the eddy viscosity (which governs the mean flow) is much larger than the molecular viscosity (which governs viscous dissipation for acoustics). This work seeks to exploit this in order to derive analytical solutions for the acoustics via matched asymptotic expansions in three scaling regions that cover an entire cylindrical acoustically lined duct.

2. Governing equations

A. Geometry and variable scaling

We consider the flow of a compressible viscous perfect fluid through an acoustically lined cylindrical duct of radius l^* (a star denotes a dimensional variable). The fluid is described by its pressure p^*, velocity vector $\mathbf{u}^* = (u^*, v^*, w^*)$, density ρ^* and temperature τ^*; these variables each have a steady mean-flow part denoted by a capital letter. With the cylindrical coordinate system (x^*, r^*, θ), the axial, non-swirling, parallel mean flow takes the form $\mathbf{U}^* = (U^*(r^*), 0, 0)$, and the mean temperature and density profiles are $T^*(r^*)$ and $D^*(r^*)$, respectively. The mean pressure P^* is assumed constant across any cross-section of the duct. No slip and isothermal wall conditions are satisfied at $r^* = l^*$.

With a subscript 0 denoting values at the duct centreline $r^* = 0$, we nondimensionalise as follows: length is scaled by l^*; velocity by the centreline speed of sound $c_0^* = \sqrt{\gamma P_0^*/D_0^*}$; time by l^*/c_0^*; density by D_0^*; pressure by $D_0^* {c_0^*}^2$; and temperature by ${c_0^*}^2/c_p^*$. The dynamic and bulk coefficients of viscosity, μ^* and μ^{B*}, are nondimensionalised by $c_0^* l^* D_0^*$, and the thermal conductivity κ^* by $c_0^* l^* D_0^* c_p^*$. With this scheme, the mean pressure takes the nondimensional value $P \equiv P_0 = 1/\gamma$, where $\gamma = c_p^*/c_v^*$ is the ratio of specific heats. At the duct centreline, the mean density and temperature take the nondimensional values $D_0 = 1$ and $T_0 = 1/(\gamma - 1)$, respectively. The dimensionless mean flow at $r = 0$ is $U_0 = M$, the centreline Mach number. The Reynolds number Re and the Prandtl number Pr are defined in terms of the centreline variables as

$$\mathrm{Re} = \frac{c_0^* l^* D_0^*}{\mu_0^*}, \qquad \mathrm{Pr} = \frac{\mu_0^* c_p^*}{\kappa_0^*}, \tag{2.1}$$

where the sound speed rather than the flow speed is used to define Re.

B. Viscous governing equations

The dynamics of a viscous, compressible, perfect fluid are governed by the Navier–Stokes equations and a constitutive law[18,19]

$$\frac{\partial \rho}{\partial t} + \nabla \cdot (\rho \mathbf{u}) = 0, \tag{2.2a}$$

$$\rho \frac{D\mathbf{u}}{Dt} = -\nabla p + \nabla \cdot \sigma, \tag{2.2b}$$

$$\rho \frac{D\tau}{Dt} = \frac{Dp}{Dt} + \nabla \cdot (\kappa \nabla \tau) + \sigma_{ij} \frac{\partial u_i}{\partial x_j}, \tag{2.2c}$$

$$\tau = \frac{\gamma}{\gamma - 1} \frac{p}{\rho}, \tag{2.2d}$$

which have been nondimensionalised using the scheme described above. The material derivative is $D/Dt = \partial/\partial t + \mathbf{u} \cdot \nabla$, and the viscous stress tensor is defined

$$\sigma_{ij} = 2\mu \left(\frac{\partial u_i}{\partial x_j} + \frac{\partial u_j}{\partial x_i} \right) + (\mu^B - \frac{2}{3}\mu) \nabla \cdot \mathbf{u} \delta_{ij}. \tag{2.3}$$

The viscosities and thermal conductivity are taken to depend linearly on the temperature:

$$\mu = \frac{\tau}{T_0 \mathrm{Re}}, \qquad \mu_B = \frac{\tau}{T_0 \mathrm{Re}} \frac{\mu_0^{B*}}{\mu_0^*}, \qquad \kappa = \frac{\tau}{T_0 \mathrm{Re}\, \mathrm{Pr}}. \tag{2.4}$$

The fluid variables are assumed to have a small fluctuating part in addition to the steady mean-flow part: $\mathbf{u} = \mathbf{U} + \epsilon_a \tilde{\mathbf{u}}_a$ for the velocity; $p = P + \epsilon_a \tilde{p}_a$ for the pressure; $\rho = D + \epsilon_a \tilde{\rho}_a$ for the density; and

$\tau = T + \epsilon_a \tilde{\tau}_a$ for the temperature. The parameter ϵ_a sets the scale of the fluctuations; we will call it the acoustic amplitude and assume that $\epsilon_a \ll 1$. Each fluctuating quantity is assigned the harmonic form $\tilde{q}_a(x, r, \theta, t) = \tilde{q}(r) \exp(i\omega t - ikx - im\theta)$ where ω is the frequency, k is the axial wavenumber and m, an integer, is the azimuthal mode number. The exponential factor will be dropped for simplicity henceforth. We will consider a single mode (ω, k, m) and calculate the radial mode shapes $\tilde{q}(r)$. The full sound field can then be reconstructed by summing over m modes and inverting the Fourier transforms for ω and k.

Linearised sound – sound for which the acoustic amplitude is small – is governed by the linearised compressible Navier–Stokes equations. These may be derived by expanding the equations (2.2) for the mean and fluctuating fluid variables and considering only those terms that are $\mathcal{O}(\epsilon_a)$:

$$\left.\begin{aligned}
&i\rho(\omega - Uk)\tilde{u} + \rho U_r \tilde{v} = ik\tilde{p} + \mathcal{V}^u, \qquad i\rho(\omega - Uk)\tilde{v} = -\tilde{p}_r + \mathcal{V}^v, \\
&i\rho(\omega - Uk)\tilde{w} = \frac{im}{r}\tilde{p} + \mathcal{V}^w, \qquad i\rho(\omega - Uk)\tilde{\tau} + \rho T_r \tilde{v} = i(\omega - Uk)\tilde{p} + \mathcal{V}^t, \\
&i\rho(\omega - Uk)\gamma\tilde{p} - i\rho^2(\omega - Uk)(\gamma - 1)\tilde{\tau} - ik\rho\tilde{u} + (\rho\tilde{v})_r + \frac{1}{r}\rho\tilde{v} - \frac{im}{r}\rho\tilde{w} = 0,
\end{aligned}\right\} \tag{2.5}$$

where a subscript denotes a derivative. The viscous terms are collected in the $\mathcal{V}^i$ terms, and are defined by

$$\begin{aligned}
\mathcal{V}^u = \frac{(\gamma-1)}{\mathrm{Re}}\Big\{&(T\tilde{u}_r + U_r\tilde{\tau})_r + \frac{1}{r}(T\tilde{u}_r + U_r\tilde{\tau}) - (2+\beta)k^2 T\tilde{u} - \frac{m^2}{r^2}T\tilde{u} \\
&- ik(1+\beta)(T\tilde{v})_r + ik\beta T_r\tilde{v} - \frac{ik}{r}(1+\beta)T\tilde{v} - \frac{km}{r}(1+\beta)T\tilde{w}\Big\},
\end{aligned} \tag{2.6a}$$

$$\begin{aligned}
\mathcal{V}^v = \frac{(\gamma-1)}{\mathrm{Re}}\Big\{&-ik(1+\beta)(T\tilde{u})_r + ik(T_r\tilde{u} - U_r\tilde{\tau}) + (2+\beta)(T\tilde{v}_r)_r - \Big(k^2 + \frac{m^2}{r^2}\Big)T\tilde{v} \\
&- \frac{2}{r}T_r\tilde{v} + (2+\beta)\Big(\frac{T\tilde{v}}{r}\Big)_r - im(1+\beta)\Big(\frac{T\tilde{w}}{r}\Big)_r + \frac{im}{r}T_r\tilde{w} + \frac{2im}{r^2}T\tilde{w}\Big\},
\end{aligned} \tag{2.6b}$$

$$\begin{aligned}
\mathcal{V}^w = \frac{(\gamma-1)}{\mathrm{Re}}\Big\{&-\frac{km}{r}(1+\beta)T\tilde{u} - \frac{im}{r^2}(3+\beta)T\tilde{v} - \frac{im}{r}(1+\beta)(T\tilde{v})_r + \frac{im}{r}\beta T_r\tilde{v} \\
&- \Big(k^2 + \frac{m^2}{r^2}\Big)T\tilde{w} + (T\tilde{w}_r)_r - \frac{m^2}{r^2}(1+\beta)T\tilde{w} + T\Big(\frac{\tilde{w}}{r}\Big)_r - \frac{1}{r}T_r\tilde{w}\Big\},
\end{aligned} \tag{2.6c}$$

$$\begin{aligned}
\mathcal{V}^t = \frac{(\gamma-1)}{\mathrm{Re}}\Big\{&\frac{1}{\mathrm{Pr}}(T\tilde{\tau})_{rr} + \frac{1}{\mathrm{Pr}\,r}(T\tilde{\tau})_r - \frac{1}{\mathrm{Pr}}\Big(k^2 + \frac{m^2}{r^2}\Big)T\tilde{\tau} + U_r^2\tilde{\tau} + 2TU_r\tilde{u}_r \\
&- 2ikTU_r\tilde{v}\Big\}.
\end{aligned} \tag{2.6d}$$

This paper is concerned with finding analytical solutions to the governing equations (2.5) in three regions of the duct cross-section in which different simplifying assumptions may be made. Results will be compared with numerical solution of the full linearised problem (2.5).

3. Three regions of the duct cross-section

A. The inviscid core

Away from the lined wall of the duct, where the mean flow may be approximated as constant ($U = M$, $D = 1$), viscous effects are usually negligible[14]. This region can be thought of as occupying $r \in [0, 1-\delta]$, where $\delta \ll 1$ is the nominal dimensionless width of the mean flow shear layer. In the inviscid limit $\mathrm{Re} \to \infty$, (2.5) reduce to the linearised Euler equations, from which the Pridmore-Brown equation[20] for the acoustic pressure may be derived:

$$\frac{\mathrm{d}^2\tilde{p}}{\mathrm{d}r^2} + \frac{1}{r}\frac{\mathrm{d}\tilde{p}}{\mathrm{d}r} + \left((\omega - Mk)^2 - k^2 - \frac{m^2}{r^2}\right)\tilde{p} = 0. \tag{3.1}$$

Equation (3.1) may be solved in terms of Bessel functions, and the Euler momentum equation $i\rho(\omega - Uk)\tilde{v} = -\tilde{p}_r$ may be used to find the acoustic radial velocity,

$$\tilde{p}_{\mathrm{u}}(r) = EJ_m(\alpha r), \qquad \tilde{v}_{\mathrm{u}}(r) = \frac{iE\alpha J_m'(\alpha r)}{\omega - Mk}, \tag{3.2}$$

where $\alpha^2 = (\omega - Mk)^2 - k^2$ and a prime denotes a derivative with respect to the argument. The expressions (3.2) form our outer solutions for the acoustic pressure and radial velocity.

Re	Blasius δ (%)	New δ (%)
10^5	0.3	2.2
10^6	0.1	1.0
10^7	0.03	0.5

Table 1. Boundary layer thicknesses as percentage of duct radius at three different Reynolds numbers for the Blasius boundary layer scaling $\mathrm{Re} \sim 1/\delta^2$, and the new scaling proposed here $\mathrm{Re} \sim 1/\delta^3$

B. The slightly viscous main boundary layer

Closer to the wall than the inviscid uniform outer flow, mean flow shear becomes important and the acoustic variables start to feel the effects of viscosity. It is thought that the Reynolds number of the flow in an aeroengine bypass duct is between 10^5 and 10^7 in-flight, and at take-off and landing. Common assumptions for the thickness δ of the boundary layer are between 0.2 and 3% of the duct radius. The classical Blasius boundary scaling states that $\mathrm{Re} \sim 1/\delta^2$; this choice of scaling underestimates the boundary layer thickness for the majority of the pertinent Reynolds number range. We propose the new scaling $\mathrm{Re} \sim 1/\delta^3$ for the main boundary layer, which models a slightly thicker boundary layer (or a slightly weaker viscosity), see table 1. This can be thought of, in broad terms, as emulating the thickening of a boundary layer during the transition to turbulence; as modelling a weak eddy viscosity outside the viscous sublayer; or simply as accounting for a region outside the viscous sublayer where molecular viscosity does not quite balance the inertia of the flow. We can think of this region as occupying $r \in [1-\delta, 1-\delta_a]$, where $\delta_a \ll \delta$ is the nominal dimensionless width of the acoustic boundary layer

The main boundary layer scaling is

$$r = 1 - \delta y, \qquad \xi\delta^3 = 1/\mathrm{Re}, \tag{3.3}$$

where y is the inner variable and $\xi = \mathcal{O}(1)$. The governing equations (2.5) are expanded in this regime, and as in[17], the acoustic temperature and axial velocity are scaled as

$$\tilde{u} = \frac{\hat{u}}{\delta}, \qquad \tilde{\tau} = \frac{\hat{\tau}}{\delta} \tag{3.4}$$

to balance the leading order of the continuity equation. The governing equations to first order in δ are

$$i(\omega - Uk)\hat{\tau} + ikT\hat{u} + T^2\left(\frac{\tilde{v}}{T}\right)_y = \delta\left[\gamma i(\omega - Uk)T\tilde{p} + T\tilde{v} - imT\tilde{w}\right], \tag{3.5a}$$

$$i(\omega - Uk)\hat{u} - U_y\tilde{v} = \delta\left[\xi(\gamma-1)^2T(T\hat{u}_y + U_y\hat{\tau})_y + i(\gamma-1)kT\tilde{p}\right], \tag{3.5b}$$

$$\tilde{p}_y = \delta\frac{i(\omega - Uk)}{(\gamma-1)T}\tilde{v}, \tag{3.5c}$$

$$\frac{i(\omega - Uk)}{(\gamma-1)^2T}\tilde{w} = \frac{im}{\gamma-1}\tilde{p} + \mathcal{O}(\delta), \tag{3.5d}$$

$$\begin{aligned} i(\omega - Uk)\hat{\tau} - T_y\tilde{v} = \delta\Big[&\frac{1}{\mathrm{Pr}}\xi(\gamma-1)^2T(T\hat{\tau})_{yy} + \xi(\gamma-1)^2T(U_y^2\hat{\tau} + 2TU_y\hat{u}_y) \\ &+(\gamma-1)i(\omega - Uk)T\tilde{p}\Big]. \end{aligned} \tag{3.5e}$$

It is clear from (3.5) that the choice of scaling (3.3) has pushed viscosity back to being a first order effect. When solving (3.5), we are calculating an inviscid leading order and subsequently finding the first order correction terms that account for both a finite boundary layer thickness and viscothermal effects.

C. The viscous sublayer

We assume the existence of a thin viscous sublayer within which the base flow does not change quickly, but the acoustics change rapidly enough to satisfy viscous wall conditions at $r = 1$, $y = 0$. We scale into the sublayer by

$$r = 1 - \delta_a z, \qquad \delta_a = \varepsilon\delta, \qquad \varepsilon = \sqrt{\delta/\omega}, \tag{3.6}$$

where z is the inner-inner variable, $\delta_a \sim \mathrm{Re}^{-1/2}$ and

$$\frac{1}{\mathrm{Re}} = \xi\omega^3\varepsilon^6 \tag{3.7}$$

with the $\mathcal{O}(1)$ quantity ξ the same as in (3.3). The sublayer may be thought of as occupying $r \in [1-\delta_a, 1]$. We may expand the base flow near the wall using the no slip and isothermal wall conditions,

$$\begin{aligned}
&U \sim \varepsilon z U'(0) + \frac{1}{2}\varepsilon^2 z^2 U''(0),\\
&U_y \sim U'(0) + \varepsilon z U''(0) + \frac{1}{2}\varepsilon^2 z^2 U'''(0),\\
&U_{yy} \sim U''(0) + \varepsilon z U'''(0) + \frac{1}{2}\varepsilon^2 z^2 U''''(0),\\
&T \sim T(0) + \frac{1}{2}\varepsilon^2 z^2 T''(0),\\
&T_y \sim \varepsilon z T''(0) + \frac{1}{2}\varepsilon^2 z^2 T'''(0),\\
&T_{yy} \sim T''(0) + \varepsilon z T'''(0) + \frac{1}{2}\varepsilon^2 z^2 T''''(0),
\end{aligned} \tag{3.8}$$

where the derivatives and arguments of the base flow variables remain in terms of y, i.e.

$$U'(0) \equiv \frac{\mathrm{d}}{\mathrm{d}y} U(y)|_{y=0}.$$

We will drop the argument 0 for all base flow variables in this section, as they will all be evaluated at the boundary: $U' \equiv U'(0)$, and so on.

Expanding (2.5) using (3.6) and (3.8) leads to the sublayer governing equations

$$\begin{aligned}
\tilde{v}_z =&\, \varepsilon\Big[-ik\hat{u} - \frac{i\omega}{T}\hat{\tau}\Big] + \varepsilon^2\Big[ik\frac{U'}{T}z\hat{\tau} + \frac{T''}{T}z\tilde{v}\Big] + \varepsilon^3\Big[(kU'' + \omega T'')\frac{i}{2T}z^2\hat{\tau}\\
&+ \frac{T'''}{2T}z^2\tilde{v} - im\omega\tilde{w} + i\gamma\omega^2\tilde{p} + \omega\tilde{v}\Big], && \text{(3.9a)}\\
\hat{u}_{zz} - \eta^2\hat{u} =&\, \frac{iU'}{\omega}\eta^2\tilde{v} - \varepsilon\Big[\frac{kU'}{\omega}\eta^2 z\hat{u} + \frac{U'}{T}\hat{\tau}_z - \frac{iU''}{\omega}\eta^2 z\tilde{v}\Big] - \varepsilon^2\Big[k\eta^2(\gamma-1)T\tilde{p} - \frac{iU'''}{2\omega}\eta^2 z^2\tilde{v}\\
&+ \frac{kU''}{2\omega}\eta^2 z^2\hat{u} + \frac{T''}{T}(z^2\hat{u}_{zz} + z\hat{u}_z) + \frac{U''}{T}(z\hat{\tau})_z\Big], && \text{(3.9b)}\\
\tilde{p}_z =&\, \varepsilon^3\Big[\frac{i\omega^2}{(\gamma-1)T}\tilde{v} - \frac{i\omega^2(2+\beta)}{(\gamma-1)\eta^2 T}\tilde{v}_{zz}\Big], && \text{(3.9c)}\\
\tilde{w}_{zz} - \eta^2\tilde{w} =& -\frac{m}{\omega}(\gamma-1)T\eta^2\tilde{p} + \mathcal{O}(\varepsilon), && \text{(3.9d)}\\
\frac{1}{\mathrm{Pr}}\hat{\tau}_{zz} - \eta^2\hat{\tau} =& -\varepsilon\Big[2U'\hat{u}_z + \frac{kU'}{\omega}\eta^2 z\hat{\tau} - \frac{iT''}{\omega}\eta^2 z\tilde{v}\Big] - \varepsilon^2\Big[(\gamma-1)T\omega\eta^2\tilde{p} - \frac{iT'''}{2\omega}\eta^2 z^2\tilde{v}\\
&+ 2U''z\hat{u}_z + \frac{kU''}{2\omega}\eta^2 z^2\hat{\tau} + \frac{U'^2}{T}\hat{\tau} + \frac{1}{\mathrm{Pr}}\frac{T''}{T}\Big((z^2\hat{\tau}_z)_z + \hat{\tau}\Big)\Big], && \text{(3.9e)}
\end{aligned}$$

where we have defined

$$\eta^2 = \frac{i}{\xi(\gamma-1)^2 T(0)^2} \tag{3.10}$$

with $\mathrm{Re}(\eta) > 0$. The $\hat{u}$, $\hat{\tau}$ and $\tilde{w}$ solutions of (3.9) will satisfy the required viscous wall conditions at $r = 1$; the $\tilde{p}$ and $\tilde{v}$ solutions will be free to either match with the main boundary layer solutions as $z \to \infty$ or satisfy an impedance boundary condition at $z = 0$.

D. Relating the boundary layers to the impedance

We are modelling the complicated physics of a resonator sheet or bulk lining as an impedance Z, which allows an acoustic pressure $\tilde{p}(1)$ to drive a wall-normal velocity $\tilde{v}(1)$, where $r = 1$ is the duct wall. Only the viscous sublayer described in section C is in contact with the wall, so the boundary condition

$$\tilde{p}_{\mathrm{s}} = Z\tilde{v}_{\mathrm{s}} \tag{3.11}$$

can only be applied to solutions of the sublayer governing equations. (The subscript s refers to the sublayer.) However, we are interested in the effective impedance Z_{eff} seen by the acoustics in the inviscid core of the duct described in section A; we can extrapolate the acoustic pressure and radial velocity to the wall at $r = 1$ to define

$$\tilde{p}_{\text{u}}(1) = Z_{\text{eff}}\tilde{v}_{\text{u}}(1). \tag{3.12}$$

We can include in the function Z_{eff} information about the boundary impedance Z, as well as the boundary layer physics.

In order to ascertain the functional form of Z_{eff}, we must solve in the viscous sublayer and the main boundary layer and asymptotically match our solutions through the three layers. Then, we will be able to write $\tilde{p}_{\text{s}}(1)$ and $\tilde{v}_{\text{s}}(1)$ as functions of $\tilde{p}_{\text{u}}(1)$ and $\tilde{v}_{\text{u}}(1)$, and use the two relations (3.11) and (3.12) to write the effective impedance Z_{eff} as a function of the boundary impedance Z (which we assume is known).

4. Solving for the sound

Having already written the solutions for the acoustic pressure and radial velocity in the inviscid core of the duct (in terms of Bessel functions) in (3.2), we proceed here with solving for the acoustics in the two inner regions.

A. Solving in the main boundary layer

Here we solve (3.5) to first order in the boundary layer thickness δ, working now in terms of y rather than r. The acoustic quantities are expanded as a power series in δ: $\tilde{q} = \tilde{q}_0 + \delta\tilde{q}_1 + \mathcal{O}(\delta^2)$. Then, at leading order, we use the relations

$$\hat{u}_0 = -\frac{iU_y}{\omega - Uk}\tilde{v}_0, \qquad \hat{\tau}_0 = -\frac{iT_y}{\omega - Uk}\tilde{v}_0 \tag{4.1}$$

from (3.5b) and (3.5e) to rearrange the continuity equation (3.5a). The continuity equation reduces to

$$T(\omega - Uk)\left(\frac{\tilde{v}_0}{\omega - Uk}\right)_y = 0, \tag{4.2}$$

which has the solution $\tilde{v}_{\text{m},0} = \bar{A}_0(\omega - Uk)$, where $\bar{A}_0$ is a constant and the subscript $\text{m},0$ denotes the leading order of the main boundary layer solution. Thus we may write $\hat{u}_{\text{m},0} = -iU_y\bar{A}_0$ and $\hat{\tau}_{\text{m},0} = -iT_y\bar{A}_0$. The pressure equation (3.5c) is readily integrated at leading order to produce $\tilde{p}_{\text{m},0} = \bar{P}_0$, a constant. We may use this in equation (3.5d) to find $\tilde{w}_{\text{m},0} = m(\gamma-1)T\bar{P}_0/(\omega - Uk)$. This is the highest order of the azimuthal acoustic velocity solution that we need for the current study. Notice that the solutions for $\hat{u}_{\text{m},0}$ and $\tilde{w}_{\text{m},0}$ cannot satisfy the no slip condition at the wall $y = 0$, as $U_y(0), T(0) \neq 0$ in general, and we must have $\bar{A}_0, \bar{P}_0 \neq 0$ for a non-trivial solution. This indicates the necessity of a viscous sublayer.

At first order, the $\hat{u}$ and $\hat{\tau}$ solutions may be written

$$\hat{u}_{\text{m},1} = -\frac{iU_y}{\omega - Uk}\tilde{v}_1 + \frac{(\gamma-1)kT}{\omega - Uk}\bar{P}_0 - \xi\bar{A}_0\frac{(\gamma-1)^2T}{\omega - Uk}(U_yT)_{yy}, \tag{4.3}$$

$$\hat{\tau}_{\text{m},1} = -\frac{iT_y}{\omega - Uk}\tilde{v}_1 + (\gamma-1)T\bar{P}_0 - \xi\bar{A}_0\frac{(\gamma-1)^2T}{\omega - Uk}\left(\frac{1}{2\text{Pr}}(T^2)_{yyy} + (TU_y^2)_y\right), \tag{4.4}$$

where the subscript 1 denotes the first order. These are used in (3.5a) which, when integrated, gives

$$\begin{aligned}\tilde{v}_{\text{m},1} = {}&\bar{A}_1(\omega - Uk) + \bar{A}_0(\omega - Uk)y + i\bar{P}_0(\omega - Uk)y\Big(1 - \frac{k^2 + m^2}{(\omega - Mk)^2}\Big)\\ &+ i\bar{P}_0(\omega - Uk)\frac{k^2 + m^2}{(\omega - Mk)^2}\int_0^y \chi_1\,\mathrm{d}y + i\xi\bar{A}_0(\gamma-1)^2(\omega - Uk)\int_0^y \bar{\chi}_\mu\,\mathrm{d}y,\end{aligned} \tag{4.5}$$

where $\bar{A}_1$ is a constant, and

$$\chi_1 = 1 - \frac{(\omega - Mk)^2}{\rho(\omega - Uk)^2}, \qquad \bar{\chi}_\mu = \frac{1}{\omega - Uk}\left(\frac{1}{2\text{Pr}}(T^2)_{yyy} + (TU_y^2)_y + \frac{kT}{\omega - Uk}(U_yT)_{yy}\right). \tag{4.6}$$

Note that viscous terms, identifiable by the parameter ξ, have arisen at this order in eqs. (4.3)–(4.5). The first order pressure is found by integrating (3.5c):

$$\tilde{p}_{\mathrm{m},1} = \bar{P}_1 + i\bar{A}_0(\omega - Mk)^2 y - i\bar{A}_0(\omega - Mk)^2 \int_0^y \chi_0 \,\mathrm{d}y, \tag{4.7}$$

where $\bar{P}_1$ is a constant, and

$$\chi_0 = 1 - \frac{\rho(\omega - Uk)^2}{(\omega - Mk)^2}. \tag{4.8}$$

In summary, the solutions for the acoustic pressure and radial velocity in the main boundary layer, correct to first order, are

$$\begin{aligned} \tilde{v}_{\mathrm{m}}(y) = (\omega - Uk)\Big\{ &\bar{A}_0 + \delta\bar{A}_1 + \delta\bar{A}_0 y + i\delta\bar{P}_0 y\Big(1 - \frac{k^2+m^2}{(\omega - Mk)^2}\Big) \\ &+ i\delta\bar{P}_0\frac{k^2+m^2}{(\omega - Mk)^2}\int_0^y \chi_1 \,\mathrm{d}y + i\delta\xi\bar{A}_0(\gamma-1)^2\int_0^y \bar{\chi}_\mu \,\mathrm{d}y\Big\}, \end{aligned} \tag{4.9a}$$

$$\tilde{p}_{\mathrm{m}}(y) = \bar{P}_0 + \delta\bar{P}_1 + i\delta\bar{A}_0(\omega - Mk)^2 y - i\delta\bar{A}_0(\omega - Mk)^2\int_0^y \chi_0 \,\mathrm{d}y. \tag{4.9b}$$

These are identical in form to the pressure and radial velocity found by Brambley [10] by assuming an inviscid, thin-but-nonzero thickness boundary layer — but for the addition of the viscous integral at first order in $\tilde{v}_{\mathrm{m}}$ (that of $\bar{\chi}_\mu$).

B. Solving in the viscous sublayer

Here we solve the system (3.9) subject to no slip and isothermal boundary conditions

$$\hat{u}_{\mathrm{s}}(0) = \hat{\tau}_{\mathrm{s}}(0) = \tilde{w}_{\mathrm{s}}(0) = 0, \tag{4.10}$$

in terms of the inner-inner variable z. To proceed, the acoustic variables are expanded in ascending powers of ε, $\tilde{q} = \tilde{q}_0 + \varepsilon\tilde{q}_1$ et cetera. Solving the governing equations to $\mathcal{O}(\varepsilon^3)$ produces expressions for the acoustic pressure and radial velocity

$$\tilde{p}_{\mathrm{s}}(z) = P_0 + \varepsilon P_1 + \varepsilon^2 P_2 + \varepsilon^3\Big(P_3 + \frac{i\omega^2}{(\gamma-1)T}A_0 z\Big), \tag{4.11a}$$

$$\begin{aligned} \tilde{v}_{\mathrm{s}}(z) = A_0 &+ \varepsilon\left[A_1 + a_0 \mathrm{e}^{-\eta z} + a_1 z\right] + \varepsilon^2\Big[A_2 + a_2 z + a_3 z^2 + (a_4 + a_5 z + a_6 z^2)\mathrm{e}^{-\eta z} + a_7 \mathrm{e}^{-\sigma\eta z}\Big] \\ &+ \varepsilon^3\Big[A_3 + a_8 z + a_9 z^2 + a_{10} z^3 + (a_{11} + a_{12} z + a_{13} z^2 + a_{14} z^3 + a_{15} z^4)\mathrm{e}^{-\eta z} \\ &+ (a_{16} + a_{17} z + a_{18} z^2)\mathrm{e}^{-\sigma\eta z}\Big], \end{aligned} \tag{4.11b}$$

where A_j and P_j are constants of integration, and a_j are linear combinations of the A_j and P_j defined in appendix A. Here, $\sigma = \sqrt{\mathrm{Pr}}$. Interestingly, (4.11) shows that $\tilde{v}_{\mathrm{s}}$ is effected by viscosity at $\mathcal{O}(\varepsilon)$, while $\tilde{p}_{\mathrm{s}}$ is inviscid to $\mathcal{O}(\varepsilon^3)$ despite the viscous term $\propto \tilde{v}_{zz}/\eta^2$ appearing at $\mathcal{O}(\varepsilon^3)$ in (3.9c).

5. Asymptotic matching and the effective impedance

A. Matching the core and main boundary layer solutions

Close to the duct wall, the inviscid core solutions (3.2) may be written in terms of the inner variable y as

$$\tilde{p}_{\mathrm{u}}^{(I)}(1 - \delta y) = p_\infty + \delta y i(\omega - Mk)v_\infty + \mathcal{O}(\delta^2), \tag{5.1a}$$

$$\tilde{v}_{\mathrm{u}}^{(I)}(1 - \delta y) = v_\infty - \delta y\left(\frac{(\omega - Mk)^2 - k^2 - m^2}{i(\omega - Mk)}p_\infty - v_\infty\right) + \mathcal{O}(\delta^2), \tag{5.1b}$$

where $p_\infty \equiv \tilde{p}_{\mathrm{u}}(1) = EJ_m(\alpha)$ and $v_\infty \equiv \tilde{v}_{\mathrm{u}}(1) = i\alpha EJ'_m(\alpha)/(\omega - Mk)$ are the wall values of the core solutions, and the superscript (I) denotes "inner".

We match (4.9) to (5.1) in the limit $y \to \infty$. At leading order we find

$$\bar{A}_0 = \frac{v_\infty}{\omega - Mk}, \qquad \bar{P}_0 = p_\infty. \tag{5.2}$$

At first order, we require the terms proportional to y in (4.9) to match with the outer solutions, while the constant terms should cancel as there are no constant terms at first order in (5.1). Thus,

$$\bar{A}_1 = -ip_\infty \frac{k^2 + m^2}{(\omega - Mk)^2} I_1 - \frac{i\xi(\gamma-1)^2}{\omega - Mk} v_\infty I_\mu, \tag{5.3a}$$

$$\bar{P}_1 = i(\omega - Mk) v_\infty I_0 \tag{5.3b}$$

where

$$I_0 = \int_0^\infty \chi_0 \, \mathrm{d}y, \qquad I_1 = \int_0^\infty \chi_1 \, \mathrm{d}y, \qquad I_\mu = \int_0^\infty \bar{\chi}_\mu \, \mathrm{d}y. \tag{5.4}$$

The viscous integral (that of $\bar{\chi}_\mu$) is bounded as $y \to \infty$ because the gradients of the base flow are zero outside the boundary layer. Now we can express the main boundary layer solutions in terms of the wall values p_∞ and v_∞ of the core solutions.

B. Matching the viscous sublayer and main boundary layer solutions

To match the inner solutions (main boundary layer) to the inner-inner solutions (viscous sublayer) we must first find the near-wall behaviour of the main boundary layer solutions. First, we expand the integrals of (4.9) in the limit $y \to 0$,

$$\int_0^y \chi_0 \, \mathrm{d}y \sim \left(1 - \frac{\rho(0)\omega^2}{(\omega - Mk)^2}\right) y, \tag{5.5a}$$

$$\int_0^y \chi_1 \, \mathrm{d}y \sim \left(1 - \frac{(\omega - Mk)^2}{\rho(0)\omega^2}\right) y, \tag{5.5b}$$

$$\int_0^y \bar{\chi}_\mu \, \mathrm{d}y \sim \frac{y}{\omega^2}\Big(kT(0)^2U'''(0) + kT(0)T''(0)U'(0) + 2\omega T(0)U'(0)U''(0) + \frac{\omega}{\mathrm{Pr}}T(0)T'''(0)\Big), \tag{5.5c}$$

where we assume the base flow is non-slipping and satisfies isothermal wall conditions, $U(0) = 0$ and $T'(0) = 0$, such that $U(y) \sim U'(0)y$ and $T(y) \sim T(0)$, and similar for their derivatives. A prime denotes a derivative with respect to y. Thus for small y the pressure and radial velocity in the main boundary layer behave like

$$\tilde{p}_{\mathrm{m}}^{(I)} \sim \bar{P}_0 + \delta\bar{P}_1 + i\delta y \bar{A}_0 \rho(0)\omega^2 + \mathcal{O}(\delta^2, \delta y^2), \tag{5.6a}$$

$$\begin{aligned}\tilde{v}_{\mathrm{m}}^{(I)} \sim\ & \bar{A}_0\left(\omega - U'(0)ky - \frac{1}{2}U''(0)ky^2\right) + \delta\bar{A}_1(\omega - U'(0)ky) + \delta\bar{A}_0\omega y + i\delta y\bar{P}_0\omega \\ & - i\delta y\bar{P}_0\frac{k^2+m^2}{\rho(0)\omega} + i\delta y\xi\bar{A}_0(\gamma-1)^2\omega\bigg(\frac{k}{\omega^2}T(0)^2U'''(0) + \frac{k}{\omega^2}T(0)T''(0)U'(0) \\ & + \frac{2}{\omega}T(0)U'(0)U''(0) + \frac{1}{\mathrm{Pr}\omega}T(0)T'''(0)\bigg) + \mathcal{O}(\delta^2, \delta y^2, y^3).\end{aligned} \tag{5.6b}$$

The outer limit of the viscous sublayer solutions are found by taking $z \to \infty$:

$$\tilde{p}_{\mathrm{s}}^{(O)} \sim P_0 + \varepsilon P_1 + \varepsilon^2 P_2 + \varepsilon^3\left(P_3 + \frac{i\omega^2}{(\gamma-1)T}A_0 z\right) + \mathcal{O}(\varepsilon^4), \tag{5.7a}$$

$$\tilde{v}_{\mathrm{s}}^{(O)} \sim A_0 + \varepsilon\left(A_1 + a_1 z\right) + \varepsilon^2\left(A_2 + a_2 z + a_3 z^2\right) + \varepsilon^3\left(A_3 + a_8 z + a_9 z^2 + a_{10} z^3\right) + \mathcal{O}(\varepsilon^4), \tag{5.7b}$$

where the exponentially small terms in (4.11) vanish in this outer limit, and the superscript (O) denotes "outer". We want to match the expressions (5.7) and (5.6).

We introduce an intermediate variable to facilitate matching. Let

$$s = y/\varepsilon^\lambda = z\varepsilon^{1-\lambda} \tag{5.8}$$

where $0 < \lambda < 1$, and we take the limit $\varepsilon \to 0$ with s held fixed. For the acoustic pressure, the main boundary layer solution in the limit $y \to 0$, (5.6a), and the sublayer solution in the limit $z \to \infty$, (5.7a), may be rephrased in terms of the intermediate variable s using (5.8). We find, as $\varepsilon \to 0$ with s held fixed,

$$\tilde{p}_{\mathrm{m}}^{(I)} = \bar{P}_0 + \varepsilon^2 \omega \bar{P}_1 + i\varepsilon^{2+\lambda} s\omega^3 \bar{A}_0 \rho(0) + \mathcal{O}(\varepsilon^4, \varepsilon^{2+2\lambda}) \tag{5.9a}$$

$$\tilde{p}_{\mathrm{s}}^{(O)} = P_0 + \varepsilon P_1 + \varepsilon^2 P_2 + \varepsilon^{2+\lambda} s \frac{i\omega^2}{(\gamma-1)T(0)} A_0 + \varepsilon^3 P_3 + \mathcal{O}(\varepsilon^4). \tag{5.9b}$$

We may identify from (5.9) that $P_0 = \bar{P}_0$ and $P_2 = \omega \bar{P}_1$. The $\mathcal{O}(\varepsilon)$ matching gives $P_1 = 0$. Because we want the matching to work for any value of the exponent $\lambda \in (0,1)$, we assert there is no balance between the $\mathcal{O}(\varepsilon^{2+2\lambda})$ error term in (5.9a) and the $\mathcal{O}(\varepsilon^3)$ term in (5.9b); hence we we may set $P_3 = 0$. Writing the outer expansion $\tilde{v}_{\mathrm{s}}^{(O)}$ of the sublayer radial velocity and the inner expansion $\tilde{v}_{\mathrm{m}}^{(I)}$ of the main boundary layer solution in terms of the matching variable s, we find, as $\varepsilon \to 0$ with s held fixed,

$$\begin{aligned}\tilde{v}_{\mathrm{m}}^{(I)} = {} & \omega \bar{A}_0 - \varepsilon^{\lambda} s k U'(0) \bar{A}_0 - \varepsilon^{2\lambda} s^2 \frac{kU''(0)}{2} \bar{A}_0 - \varepsilon^{3\lambda} s^3 \frac{kU'''(0)}{6} \bar{A}_0 + \varepsilon^2 \omega^2 \bar{A}_1 + \varepsilon^{2+\lambda} s \bigg\{ \omega^2 \bar{A}_0 \\ & - kU'(0)\omega \bar{A}_1 + i\omega^2 \bar{P}_0 - i\frac{k^2+m^2}{\rho(0)} \bar{P}_0 + i\xi(\gamma-1)^2 T(0)^2 \omega \bar{A}_0 \bigg(\frac{kU'''(0)}{\omega} + \frac{kT''(0)U'(0)}{\omega T(0)} \\ & + \frac{2U'(0)U''(0)}{T(0)} + \frac{1}{\mathrm{Pr}} \frac{T'''(0)}{T(0)} \bigg) \bigg\} + \mathcal{O}(\varepsilon^{2+2\lambda}, \varepsilon^{4\lambda}),\end{aligned} \tag{5.10a}$$

$$\begin{aligned}\tilde{v}_{\mathrm{s}}^{(O)} = {} & A_0 - \varepsilon^{\lambda} s \frac{kU'(0)}{\omega} A_0 + \varepsilon A_1 - \varepsilon^{2\lambda} s^2 \frac{kU''(0)}{2\omega} A_0 - \varepsilon^{3\lambda} s^3 \frac{kU'''(0)}{6\omega} A_0 - \varepsilon^{1+\lambda} s \frac{U'(0)k}{\omega} A_1 + \varepsilon^2 A_2 \\ & - \varepsilon^{1+2\lambda} s^2 \frac{kU''(0)}{2\omega} A_1 + \varepsilon^{2+\lambda} s \bigg\{ \omega A_0 + i\omega^2 P_0 - i(k^2+m^2)(\gamma-1)T(0)P_0 - \frac{kU'(0)}{\omega} A_2 \\ & - \frac{1}{\eta^2} A_0 \bigg(\frac{T'''(0)}{\mathrm{Pr}T(0)} + \frac{2U'(0)U''(0)}{T(0)} + \frac{kT''(0)U'(0)}{\omega T(0)} + \frac{kU'''(0)}{\omega} \bigg) \bigg\} + \varepsilon^3 A_3 + \mathcal{O}(\varepsilon^4).\end{aligned} \tag{5.10b}$$

From the leading orders of (5.10a) and (5.10b) we can readily identify $A_0 = \omega \bar{A}_0$. This is consistent with higher order terms of (5.10), and also with the $\mathcal{O}(\varepsilon^{2+\lambda})$ terms in the $\tilde{p}$ expansions (5.9) once we write $\rho(0) = 1/(\gamma-1)T(0)$. At $\mathcal{O}(\varepsilon^2)$ in (5.10) we find $A_2 = \omega^2 \bar{A}_1$. Due to the absence of ε and ε^3 terms in (5.10a), we set $A_1 = A_3 = 0$. The remaining terms at $\mathcal{O}(\varepsilon^{2+\lambda})$ match gratifyingly if the definition of η is inserted from (3.10).

We can use the information gleaned from matching the main boundary layer solution to the core flow in (5.2) and (5.3) to write the sublayer constants A_j, P_j in terms of the core solution wall values p_∞ and v_∞:

$$\begin{aligned} & P_0 = p_\infty, \qquad P_2 = i\omega(\omega - Mk) I_0 v_\infty, \qquad A_0 = \frac{\omega}{\omega - Mk} v_\infty, \\ & A_2 = -i\omega^2 \frac{k^2+m^2}{(\omega-Mk)^2} I_1 p_\infty - i\xi\omega(\gamma-1)^2 I_\mu \frac{\omega}{\omega - Mk} v_\infty, \end{aligned} \tag{5.11}$$

where I_0, I_1 and I_μ are defined in (5.4). The relations (5.11) will be used in the next section to form the impedance boundary condition.

We note here that if, instead of matching to a uniform inviscid flow solution outside the boundary layer, we wanted to apply boundary conditions at the lined wall (such as a known impedance), the boundary conditions could be applied directly to the sublayer solutions at each order to ascertain the unknown coefficients. The main boundary layer solution could then be matched inwards to these known coefficients (which may require $\bar{P}_j$ and $\bar{A}_j$ to have expansions in ε), and a full solution, normalized by the wall boundary conditions, could be attained.

C. Forming the effective impedance

At the boundary, $\tilde{v}$ is

$$\tilde{v}(0) = A_0 + \varepsilon(A_1 + a_0) + \varepsilon^2(A_2 + a_4 + a_7) + \varepsilon^3(A_3 + a_{11} + a_{16}), \tag{5.12}$$

In which we set $A_1 = A_3 = 0$ as per the matching with the outer solution in the previous section. We may split a_{11}, a_{16} and A_2 up into terms proportional to v_∞ and p_∞. Then we may write

$$\tilde{v}(0) = \frac{\omega}{\omega - Mk} v_\infty \left(1 + \varepsilon S_0 + \varepsilon^2 S_1 + \varepsilon^3 S_2\right) + p_\infty \left(\varepsilon^2 S_3 + \varepsilon^3 S_4\right), \tag{5.13}$$

where

$$\begin{aligned}
S_0 &= -\frac{kU'(0)}{\omega\eta}, \\
S_1 &= -i\xi\omega(\gamma-1)^2 I_\mu + \frac{\sigma}{1+\sigma}\frac{2U'(0)^2}{\eta^2 T(0)} - \frac{5k^2U'(0)^2}{4\omega^2\eta^2}, \\
S_2 &= i\xi(\gamma-1)^2\frac{kU'(0)}{\eta} I_\mu - \frac{13k^2U'(0)U''(0)}{8\omega^2\eta^3} - \frac{kU'''(0)}{\omega\eta^3} - \frac{T'''(0)}{\sigma^3\eta^3 T(0)} - \frac{151k^3U'(0)^3}{32\omega^3\eta^3} \\
&\quad + \frac{(7\sigma+3)}{(1+\sigma)^2}\frac{kU'(0)^3}{2\omega\eta^3 T(0)} + \frac{2(\sigma^3+\sigma^2-2\sigma-1)}{\sigma(1+\sigma)^2}\frac{U'(0)T''(0)}{\omega\eta^3 T(0)} - \frac{(2\sigma^2+4\sigma+1)}{(1+\sigma)^2}\frac{kU'(0)T''(0)}{\omega\eta^3 T(0)} \\
S_3 &= -i\omega^2\frac{k^2+m^2}{(\omega-Mk)^2} I_1, \\
S_4 &= i\omega\frac{k^2+m^2}{(\omega-Mk)^2}\frac{kU'(0)}{\eta} I_1 - i(\gamma-1)(k^2+m^2)\frac{T(0)}{\eta} - \frac{i(\gamma-1)\omega^2}{\sigma\eta}.
\end{aligned}$$

Similarly, we may write $\tilde{p}$ at $z = 0$:

$$\tilde{p}(0) = p_\infty + \varepsilon^2 i\omega(\omega - Mk) I_0 v_\infty \tag{5.14}$$

Then, we use the definition of the boundary impedance, $Z = \tilde{p}(0)/\tilde{v}(0)$, and divide top and bottom by v_∞ to form the ratio for the effective impedance $Z_{\text{eff}} = p_\infty/v_\infty$:

$$Z = \frac{Z_{\text{eff}} + \varepsilon^2 i\omega(\omega - Mk)I_0}{\frac{\omega}{\omega-Mk}\left(1 + \varepsilon S_0 + \varepsilon^2 S_1 + \varepsilon^3 S_2\right) + Z_{\text{eff}}\left(\varepsilon^2 S_3 + \varepsilon^3 S_4\right)}. \tag{5.15}$$

Rearranging, and writing in terms of r and primitive variables, then gives us our effective impedance in terms of the boundary impedance Z,

$$Z_{\text{eff}} = \frac{\omega}{\omega - Mk}\frac{Z + \frac{(\gamma-1)T(1)}{\sqrt{i\omega\text{Re}}}\frac{kU_r(1)}{\omega}Z - \frac{i}{\omega}(\omega-Mk)^2\delta I_0 + (\bar{S}_1 + \bar{S}_2)Z}{1 + i(k^2+m^2)\frac{\omega Z}{(\omega-Mk)\delta I_1} - \bar{S}_4 Z} + \mathcal{O}(\delta^2), \tag{5.16}$$

where

$$\bar{S}_1 = \frac{(\gamma-1)^2}{i\omega\text{Re}}\left(\frac{I_\mu}{\delta^2} + \frac{\sigma}{1+\sigma}2U_r(1)^2T(1) - \frac{5k^2}{4\omega^2}U_r(1)^2T(1)^2\right), \tag{5.17a}$$

$$\bar{S}_2 = \frac{(\gamma-1)^3T(1)}{(i\omega\text{Re})^{3/2}}\left(\frac{kU_r(1)}{\omega}\frac{I_\mu}{\delta^2} + \frac{13k^2}{8\omega^2}U_r(1)U_{rr}(1)T(1)^2 + \frac{k}{\omega}U_{rrr}(1)T(1)^2 + \frac{T_{rrr}(1)T(1)}{\sigma^3}\right. \tag{5.17b}$$

$$+ \frac{151k^3}{32\omega^3}U_r(1)^3T(1)^2 - \frac{(7\sigma+3)}{(1+\sigma)^2}\frac{k}{2\omega}U_r(1)^3T(1) - \frac{(\sigma^3+\sigma^2-2\sigma-1)}{\sigma(1+\sigma)^2}\frac{2}{\omega}U_r(1)T_{rr}(1)T(1) \tag{5.17c}$$

$$\left. + \frac{(2\sigma^2+4\sigma+1)}{(1+\sigma)^2}\frac{k}{\omega}U_r(1)T_{rr}(1)T(1)\right) \tag{5.17d}$$

$$\bar{S}_4 = \frac{(\gamma-1)^2T(1)}{i\omega\sqrt{i\omega\text{Re}}}\left(\frac{k^2+m^2}{(\omega-Mk)^2}\frac{k\omega U_r(1)}{(\gamma-1)}\delta I_1 + \frac{\omega^2}{\sigma} + T(1)(k^2+m^2)\right), \tag{5.17e}$$

and

$$\delta I_0 = \int_0^1 1 - \frac{\rho(r)(\omega - U(r)k)^2}{(\omega-Mk)^2}\mathrm{d}r, \qquad \delta I_1 = \int_0^1 1 - \frac{(\omega-Mk)^2}{\rho(r)(\omega-U(r)k)^2}\mathrm{d}r. \tag{5.18a}$$

$$\frac{I_\mu}{\delta^2} = \int_0^1 \frac{\chi_\mu}{\delta^3}\mathrm{d}r, \qquad \frac{\chi_\mu}{\delta^3} = \frac{-\omega}{\omega - Uk}\left(\frac{1}{2\text{Pr}}(T^2)_{rrr} + (TU_r^2)_r + \frac{kT}{\omega - Uk}(U_rT)_{rr}\right) \tag{5.18b}$$

This is the main result of this paper, and provides an effective impedance Z_{eff} to be applied to inviscid plug flow acoustics that accounts for the effect of the viscous boundary layer over a lining. The error plot fig. 1 shows that the effective impedance (5.16) is correct to the stated order of accuracy.

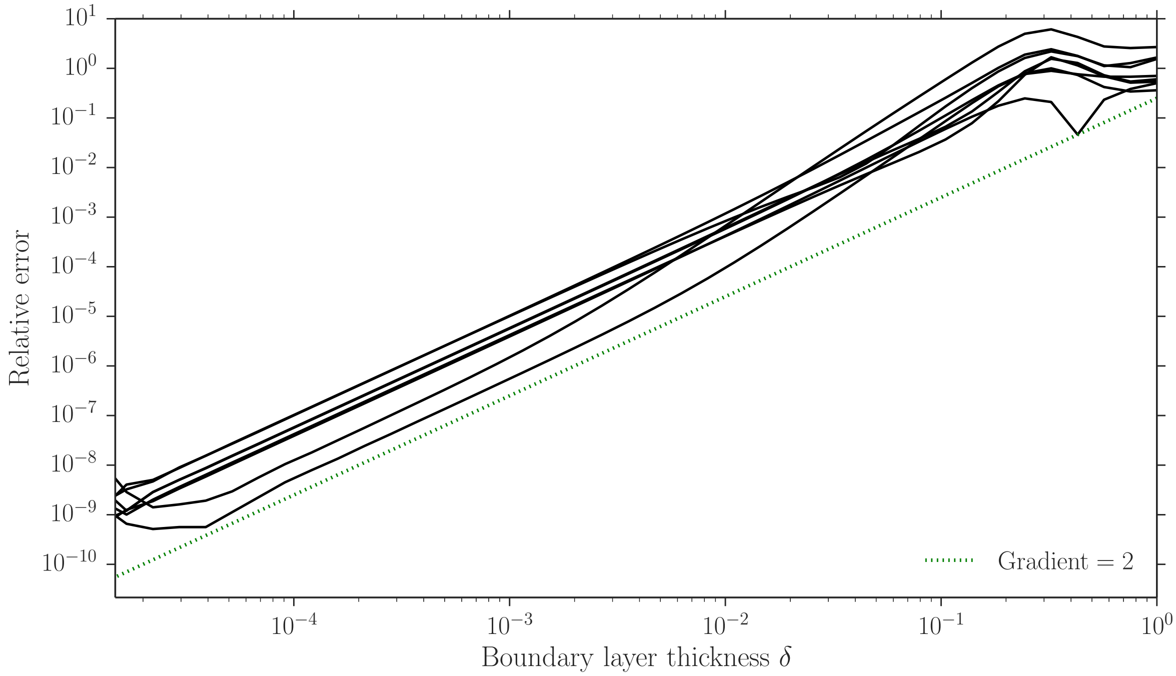

Figure 1. Asymptotic accuracy plot with relative error defined as $|Z_{\text{eff}}(Z)/(\tilde{p}_u(1)/\tilde{v}_u(1)) - 1|$, where the function $Z_{\text{eff}}(Z)$ is the asymptotic effective impedance from (5.16) with the input boundary impedance Z taken from numerical solutions of the LNSE (2.5). $k = \pm 1 \pm i$, ± 1, $\pm i$ and $\omega = 5$, $m = 0$, $M = 0.5$, $\mathrm{Re} = 1/\delta^3$. The hyperbolic base flow (6.1) is used.

6. Results

All results presented here are for a hyperbolic velocity and temperature profile,

$$U(r) = M \tanh\left(\frac{1-r}{\delta}\right) + M\left(1 - \tanh\left(\frac{1}{\delta}\right)\right)\left(\frac{1+\tanh(1/\delta)}{\delta} r + (1+r)\right)(1-r) \tag{6.1a}$$

$$T(r) = T_0 + T_{\mathrm{w}}\left(\cosh\left(\frac{1-r}{\delta}\right)\right)^{-1}, \tag{6.1b}$$

where δ is a measure of boundary layer thickness, with $U(1-3\delta) \approx 0.995M$. We take $T_{\mathrm{w}} = 0.104$ to three significant figures in what follows, to model a compressible Blasius temperature profile.

First we show some examples of the acoustic mode shapes that result from the three different duct regions considered in the asymptotic analysis. The patchwork of regions of validity for the radial velocity can be seen in fig. 2; the uniform flow outer solution $\tilde{v}_{\mathrm{u}}$ is valid for most of the duct, where the shear is negligible (see fig. 2a); the main boundary layer solution $\tilde{v}_{\mathrm{m}}$ is accurate where the mean flow shear is important, but loses accuracy very close to the wall (see fig. 2b); the viscous sublayer solution $\tilde{v}_{\mathrm{s}}$ is accurate in the acoustic boundary layer very close to the wall. For the axial velocity we see a similar thing (fig. 3), except here the viscous sublayer solution is significantly different from the main boundary layer solution due to the sublayer solution satisfying no slip at the wall.

A. Duct modes

To find duct modes of our new effective impedance boundary condition, we must first choose a model for the acoustic liner impedance. Here, we use a mass–spring–damper boundary with a mass d, spring constant b and damping coefficient R, which gives the impedance

$$Z(\omega) = R + i\omega d - ib/\omega. \tag{6.2}$$

A dispersion relation must then be satisfied,

$$Z_{\text{eff}}(Z) = \frac{\tilde{p}_u(1)}{\tilde{v}_u(1)}, \tag{6.3}$$

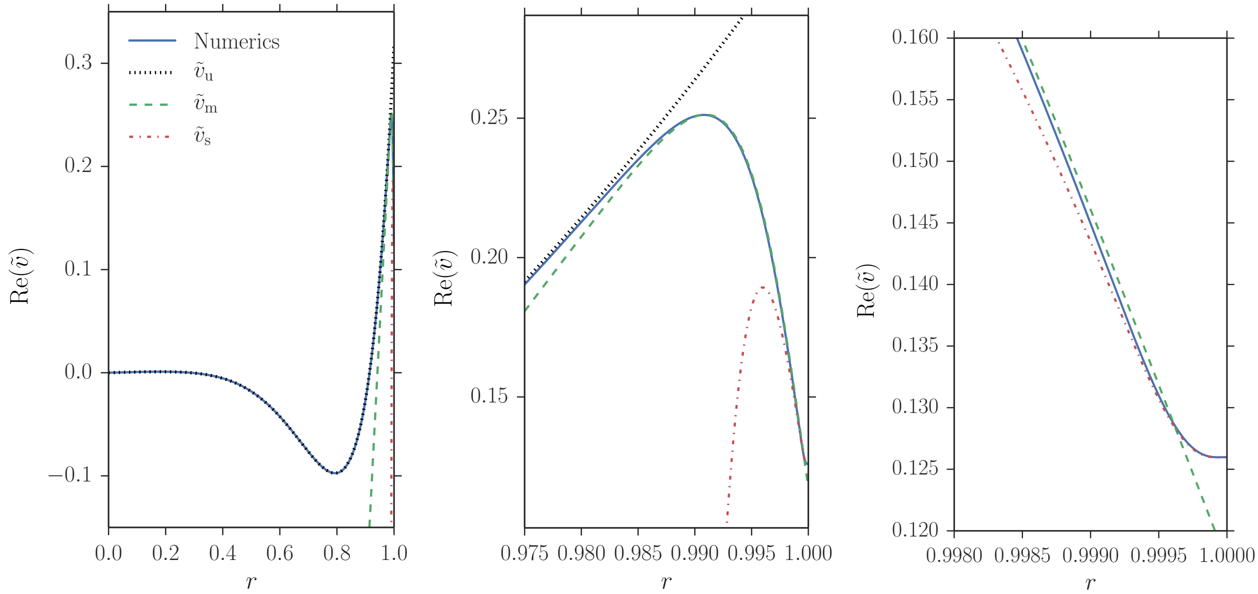

(a) (b) (c)

Figure 2. Acoustic mode shape for the radial velocity $\tilde{v}$ found by numerically solving the LNSE, with the three asymptotic solutions overlayed, showing their patchwork of regions of validity. (a) shows the full duct $r \in [0, 1]$, (b) shows the main boundary layer, (c) shows the viscous sublayer. Parameters are $\omega = 5$, $k = -14 + 5i$, $m = 0$, $M = 0.5$, $\delta = 6 \times 10^{-3}$, $\mathrm{Re} = 5 \times 10^6$.

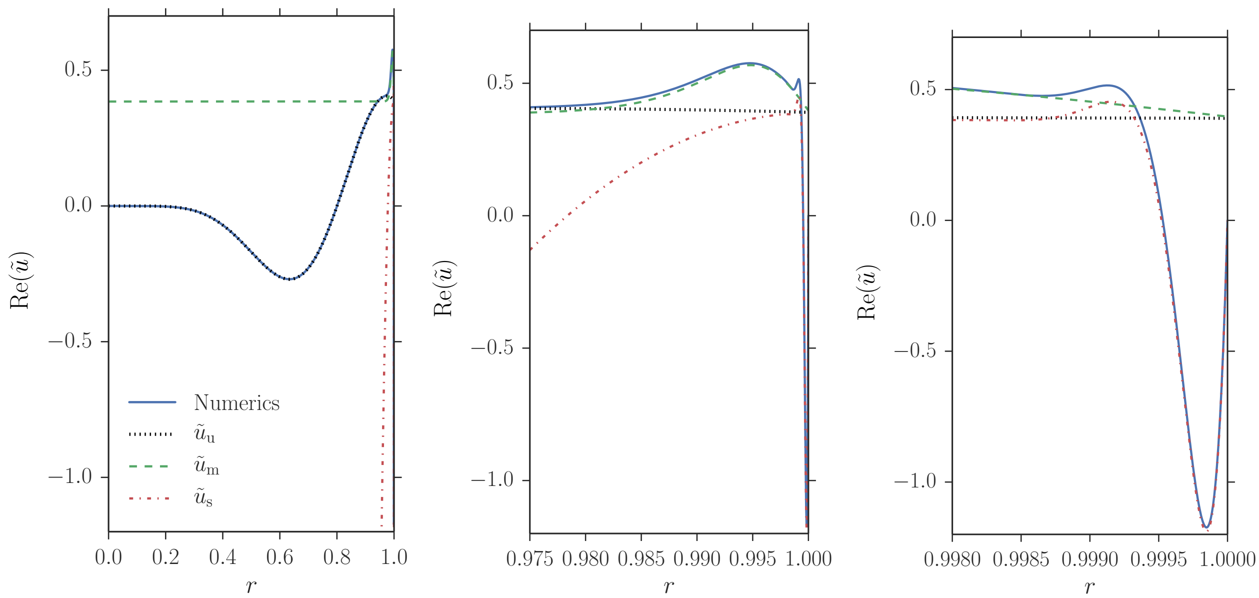

(a) (b) (c)

Figure 3. Acoustic mode shape for the axial velocity $\tilde{u}$ found by numerically solving the LNSE, with the three asymptotic solutions overlayed, showing their patchwork of regions of validity. (a) shows the full duct $r \in [0, 1]$, (b) shows the main boundary layer, (c) shows the viscous sublayer. Parameters are $\omega = 15$, $k = 5 + 2i$, $m = 6$, $M = 0.5$, $\delta = 7 \times 10^{-3}$, $\mathrm{Re} = 3 \times 10^6$.

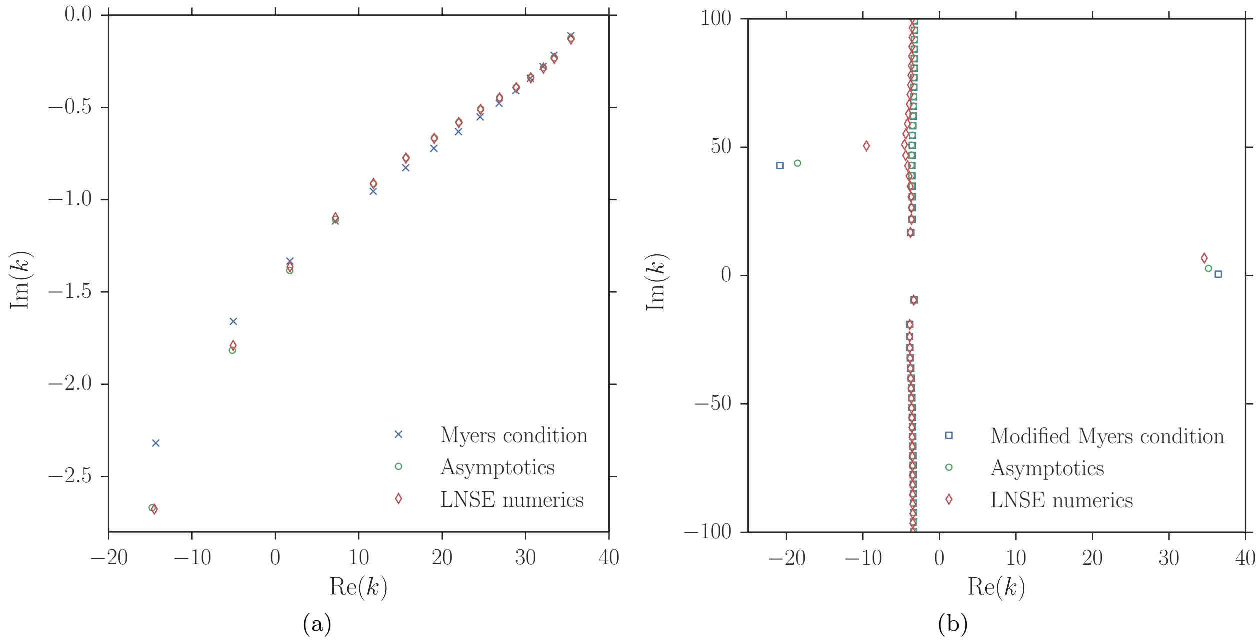

Figure 4. Duct modes in the complex k-plane. (a) shows cuton modes of the Myers boundary condition (6.4), new asymptotic condition (5.16), and numerical solution of the LNSE (2.5) for $\omega = 56$, $m = 2$, $M = 0.5$, $\delta = 8 \times 10^{-3}$, $\mathrm{Re} = 2 \times 10^6$ and a mass–spring–damper impedance (6.2) with mass $d = 0.01$, spring constant $b = 10$ and damping $R = 0.75$. (b) shows cutoff modes and two surface wave modes for the Modified Myers condition (6.5), new asymptotic condition (5.16), and numerical solution of the LNSE (2.5) for $\omega = 5$, $m = 12$, $M = 0.5$, $\delta = 7 \times 10^{-3}$, $\mathrm{Re} = 3 \times 10^6$ and a mass–spring–damper impedance (6.2) with mass $d = 0.08$, spring constant $b = 6$ and damping $R = 1.6$.

to find values of k (or ω) when ω (or k) is specified (given m). This relation comes from our definition of the effective impedance as that impedance seen by the uniform inviscid solution at the wall. The function $Z_{\text{eff}}(Z)$ is the asymptotic effective impedance with the input boundary impedance Z from (6.2). Examples of existing effective impedance boundary conditions are the Myers boundary condition[21,22], which may be written

$$Z_{\text{eff}} = \frac{\omega}{\omega - Mk} Z, \tag{6.4}$$

and its first order correction[10] (called the Modified Myers condition here),

$$Z_{\text{eff}} = \frac{\omega}{\omega - Mk} \frac{Z - \frac{i}{\omega}(\omega - Mk)^2 \delta I_0}{1 + i(k^2 + m^2)\frac{\omega Z}{(\omega - Mk)^2}\delta I_1}, \tag{6.5}$$

where δI_0 and δI_1 are as defined in (5.18). We will compare the new boundary condition (5.16) against these existing conditions, as well as against numerical solutions of the LNSE.

In fig. 4 a frequency is specified and (6.3) is solved to find allowed values of the axial wavenumber k. Figure 4a shows the downstream propagating cuton modes for the new asymptotic model (5.16), the Myers condition (6.4), and the viscous numerics (2.5). The damping of these propagating modes is predicted poorly by the Myers condition, which would lead to large errors in sound attenuation computations. The new boundary condition (5.16) is shown to predict the damping of these modes well when compared with the viscous numerics. In fig. 4b we focus on surface wave modes (those modes which exist only close to the lining), for which the Myers condition is unsuitable. We therefore plot results for the Modified Myers condition (6.5) to compare to our new condition, as the first order correction accounts for a finite layer of shear within which the surface modes may exist. The new boundary condition is predicting surface wave modes in the correct areas of the k-plane, but without impressive accuracy. We do see, however, improvement over the inviscid Modified Myers boundary condition due to the fact that the new condition accounts for the viscous sublayer and a small amount of viscosity in the main boundary layer.

7. Conclusion

With the goal of finding an analytically soluble model of acoustics in a sheared, viscous boundary layer above an acoustic lining, a weakly-viscous scaling law is adopted in the majority of the mean flow boundary layer. This region lies between an inviscid, uniform flow region outside the boundary layer, and a viscous sublayer very close to the lined wall within which the mean flow varies slowly. Analytical solutions are found each region. By asymptotically matching the solutions in the three regions, an effective impedance boundary condition may be formed, applicable to an inviscid plug flow at the wall.

Preliminary results show that duct modes of the linearised compressible Navier–Stokes equations (LNSE) are well-predicted by the new model. In particular, the damping of cuton modes — badly predicted by the Myers boundary condition — is accurately captured by the new boundary condition. Also, the position of surface wave modes (those that oscillate close to the lined wall and decay into the core of the duct) are predicted by the new model with better accuracy than the first-order-accurate inviscid Modified Myers condition. Viscosity takes effect close to the wall, precisely where the surface waves exist, so accounting for viscosity in this region is important for their accurate prediction.

A. Sublayer solution coefficients

Below are the definitions of the a_j used in the acoustic radial velocity solution in the viscous sublayer, (4.11b):

$$a_0 = -\frac{kU'}{\omega\eta}A_0, \qquad a_1 = -\frac{kU'}{\omega}A_0, \qquad a_2 = -ikb_0, \qquad a_3 = -\frac{kU''}{2\omega}A_0,$$

$$a_4 = \Big(-\frac{5}{4}\frac{k^2U'^2}{\omega^2\eta^2} - \frac{\mathrm{Pr}}{1-\mathrm{Pr}}\frac{2U'^2}{\eta^2 T}\Big)A_0 + \frac{ik}{\eta}B_1), \qquad a_5 = -\frac{5}{4}\frac{k^2U'^2}{\omega^2\eta}A_0, \qquad a_6 = -\frac{k^2U'^2}{4\omega^2}A_0,$$

$$a_7 = \frac{\mathrm{Pr}}{1-\mathrm{Pr}}\frac{2U'^2}{\sigma\eta^2 T}A_0, \qquad a_9 = -\frac{kU''}{2\omega}A_1, \qquad a_{10} = -\frac{kU'''}{6\omega}A_0,$$

$$a_{14} = -\frac{A_0kU'}{48T\omega^3}\left(17k^2TU'^2 + 4kTU''\omega + 8T''\omega^2\right), \qquad a_{15} = -\frac{A_0\eta k^3U'^3}{32\omega^3},$$

$$a_{16} = -\frac{3A_0\eta^3kTU'^3\omega}{2(\mathrm{Pr}-1)} + \frac{iD_2\eta^5T\omega^3}{\sigma}, \qquad a_{17} = -\frac{\sigma}{1-\mathrm{Pr}}\frac{A_0kU'^3}{2\eta^2T\omega}, \qquad a_{18} = \frac{\mathrm{Pr}}{1-\mathrm{Pr}}\frac{A_0kU'^3}{2\eta T\omega},$$

$$a_8 = \Big(i\omega^2 - i(k^2+m^2)(\gamma-1)T\Big)P_0 + \Big(-\frac{T'''}{\eta^2\mathrm{Pr}T} - \frac{2U'U''}{\eta^2T} - \frac{kT''U'}{\eta^2\omega T} - \frac{kU'''}{\eta^2\omega} + \omega\Big)A_0 - \frac{kU'}{\omega}A_2,$$

$$a_{11} = -A_0U'\left(\frac{151k^3U'^2}{32\eta^3\omega^3} + \frac{13k^2U''}{8\eta^3\omega^2} + \frac{k\mathrm{Pr}\left((\mathrm{Pr}-3)T''+4U'^2\right)}{\eta^3(\mathrm{Pr}-1)^2T\omega} - \frac{2(\mathrm{Pr}-3)\mathrm{Pr}U''}{\eta^3(\mathrm{Pr}-1)^2T}\right)$$
$$+8i\eta(\mathrm{Pr}-1)\omega^2\left(B_1U'\left(5k^2(\mathrm{Pr}-1)T - \frac{\mathrm{Pr}}{4\eta^3(\mathrm{Pr}-1)^2T\omega}\right) + \frac{B_2k-(\gamma-1)m^2P_0T}{8\eta^2(\mathrm{Pr}-1)\omega^2}\right),$$

$$a_{12} = U'\left(\frac{k\left(A_0\mathrm{Pr}\left(6U'^2-4T''\right)+\frac{5iB_1k}{32\eta\omega^3}\right)}{4\eta^2(\mathrm{Pr}-1)T\omega} - \frac{151A_0k^3U'^2}{32\eta^2\omega^3} - \frac{13A_0k^2U''}{8\eta^2\omega^2} + \frac{2A_0\mathrm{Pr}U''}{\eta^2(\mathrm{Pr}-1)T}\right),$$

$$a_{13} = kU'\left(8\omega^2\left(\frac{A_0\left(-\mathrm{Pr}T''+\mathrm{Pr}U'^2+T''\right)}{16\eta(\mathrm{Pr}-1)T\omega^3} + \frac{iB_1k}{32\omega^3}\right) - \frac{55A_0k^2U'^2}{32\eta\omega^3} - \frac{5A_0kU''}{8\eta\omega^2}\right),$$

where

$$B_1 = \frac{iU'}{\omega}A_1, \qquad B_2 = \Big(\frac{iU'T''}{\omega\eta^2T} + \frac{iU'''}{\omega\eta^2}\Big)A_0 - k(\gamma-1)TP_0 + \frac{iU'}{\omega}A_2 + \frac{\mathrm{Pr}}{1-\mathrm{Pr}}\frac{2iU'^3}{\omega\sigma\eta^2T}A_0,$$

$$D_2 = \Big(2U'U'' + \frac{T'''}{\mathrm{Pr}}\Big)\frac{iA_0}{\eta^2\omega} - (\gamma-1)T\omega P_0 - \frac{\mathrm{Pr}}{1-\mathrm{Pr}}\left(\Big((5+3\mathrm{Pr})\frac{ikU'^3}{2\omega^2\eta^2} + \frac{4iU'U''}{\omega\eta^2} - \frac{2ikU'T''}{\omega^2\eta^2}\Big)\frac{A_0}{1-\mathrm{Pr}} + \frac{2U'}{\eta}B_1\right).$$

References

[1] Rice, E. J., "Propagation of Waves in an Acoustically Lined Duct with a Mean Flow," *NASA Special Publication*, Vol. 207, 1969, pp. 345.

[2] Ko, S.-H., "Sound Attenuation in Lined Rectangular Ducts with Flow and Its Application to the Reduction of Aircraft Engine Noise," *Acoustical Society of America Journal*, Vol. 50, 1971, pp. 1418–1432.

[3] Tack, D. H. and Lambert, R. F., "Influence of Shear Flow on Sound Attenuation in a Lined Duct," *The Journal of the Acoustical Society of America*, Vol. 38, No. 4, 1965, pp. 655–666.

[4] Mungur, P. and Gladwell, G. M. L., "Acoustic wave propagation in a sheared fluid contained in a duct," *Journal of Sound and Vibration*, Vol. 9, No. 1, 1969, pp. 28–48.

[5] Ko, S.-H., "Sound attenuation in acoustically lined circular ducts in the presence of uniform flow and shear flow," *Journal of Sound and Vibration*, Vol. 22, No. 2, 1972, pp. 193–210.

[6] Renou, Y. and Aurégan, Y., "Failure of the Ingard-Myers boundary condition for a lined duct: An experimental investigation," *Journal of the Acoustical Society of America*, Vol. 130, No. 1, 2011, pp. 52–60.

[7] Burak, M. O., Billson, M., Eriksson, L.-E., and Baralon, S., "Validation of a Time- and Frequency-Domain Grazing Flow Acoustic Liner Model," *AIAA Journal*, Vol. 47, No. 8, 2009, pp. 1841–1848.

[8] Rienstra, S. W., "A Classification of Duct Modes Based on Surface Waves," *Wave Motion*, Vol. 37, No. 2, 2003, pp. 119–135.

[9] Brambley, E. J., "Surface modes in sheared boundary layers over impedance linings," *Journal of Sound and Vibration*, Vol. 332, 2013, pp. 3750–3767.

[10] Brambley, E. J., "Well-Posed Boundary Condition for Acoustic Liners in Straight Ducts with Flow," *AIAA Journal*, Vol. 49, No. 6, 2011, pp. 1272–1282.

[11] Rienstra, S. W. and Darau, M., "Boundary-layer thickness effects of the hydrodynamic instability along an impedance wall," *Journal of Fluid Mechanics*, Vol. 671, 2011, pp. 559–573.

[12] Aurégan, Y. and Leroux, M., "Experimental evidence of an instability over an impedance wall in a duct with flow," *Journal of Sound and Vibration*, Vol. 317, 2008, pp. 432–439.

[13] Marx, D., Aurégan, Y., Bailliet, H., and Valiére, J.-C., "PIV and LDV evidence of hydrodynamic instability over a liner in a duct with flow," *Journal of Sound and Vibration*, Vol. 329, 2010, pp. 3798–3812.

[14] Khamis, D. and Brambley, E. J., "The Effective Impedance of a Finite-Thickness Viscothermal Boundary Layer Over an Acoustic Lining," *21st AIAA/CEAS Aeroacoustics Conference and Exhibit*, American Institute of Aeronautics and Astronautics, June 2015.

[15] Nayfeh, A. H., "Effect of the acoustic boundary layer on the wave propagation in ducts," *J. Acoust. Soc. Am.*, Vol. 54, 1973, pp. 1737–1742.

[16] Aurégan, Y., Starobinski, R., and Pagneux, V., "Influence of grazing flow and dissipation effects on the acoustic boundary conditions at a lined wall," *The Journal of the Acoustical Society of America*, Vol. 109, No. 1, 2001, pp. 59–64.

[17] Brambley, E. J., "Acoustic implications of a thin viscous boundary layer over a compliant surface or permeable liner," *Journal of Fluid Mechanics*, Vol. 678, 7 2011, pp. 348–378.

[18] Landau, L. D. and Lifshitz, E. M., *Fluid Mechanics*, Elsevier, New York, 2nd ed., 1987.

[19] Stewart, H. J., "The Energy Equation for a Viscous Compressible Fluid," *Proc Natl Acad Sci USA*, Vol. 28, No. 5, 1942, pp. 161–164.

[20] Pridmore-Brown, D. C., "Sound Propagation in a Fluid Flowing Through an Attenuating Duct," *Journal of Fluid Mechanics*, Vol. 4, No. 4, 1958, pp. 393–406.

[21] Ingard, U., "Influence of fluid motion past a plane boundary on sound reflection, absorption, and transmission," *Journal of the Acoustical Society of America*, Vol. 31, 1959, pp. 1035–1036.

[22] Myers, M. K., "On the acoustic boundary condition in the presence of flow," *Journal of Sound and Vibration*, Vol. 71, No. 3, 1980, pp. 429–434.